World Academy of Science, Engineering and Technology
International Journal of Aerospace and Mechanical Engineering
Vol:8, No:6, 2014

Enhanced Method of Conceptual Sizing of Aircraft Electro-Thermal De-icing System

Ahmed Shinkafi, Craig Lawson

***Abstract*—**There is a great advancement towards the All-Electric Aircraft (AEA) technology. The AEA concept assumes that all aircraft systems will be integrated into one electrical power source in the future. The principle of the electro-thermal system is to transfer the energy required for anti/de-icing to the protected areas in electrical form. However, powering a large aircraft anti-icing system electrically could be quite excessive in cost and system weight. Hence, maximising the anti/de-icing efficiency of the electro-thermal system in order to minimise its power demand has become crucial to electro-thermal de-icing system sizing. In this work, an enhanced methodology has been developed for conceptual sizing of aircraft electro-thermal de-icing System. The work factored those critical terms overlooked in previous studies which were critical to de-icing energy consumption. A case study of a typical large aircraft wing de-icing was used to test and validate the model. The model was used to optimise the system performance by a trade-off between the de-icing peak power and system energy consumption. The optimum melting surface temperatures and energy flux predicted enabled the reduction in the power required for de-icing. The weight penalty associated with electro-thermal anti-icing/de-icing method could be eliminated using this method without under estimating the de-icing power requirement.

***Keywords*—**Aircraft de-icing system, electro-thermal, in-flight icing.

NOMENCLATURE

LWC	Liquid Water Content (g/m^3)
MVD	Mean Volumetric Diameter (μm)
T_s	Skin temperature (°C)
T_∞	Ambient temperature (°C)
T_m	Melting temperature (°C)
h_s	Skin Heat transfer coefficient (W/K.m^2)
c, C_p	Specific heat (J/kg.K)
μ	Absolute viscosity of air (kg/s.m)
λ, k_0	Thermal conductivity of air (W/m.K)
x	Characteristic length (m)
E_m	Overall collection efficiency (%)
ρ	Density (kg/m3)
$\dot{m}_{ice}$	Icing rate (kg/s)
d	Ice thickness (mm)
$\Delta L_{f\,ice}$	Latent heat of fusion of ice (kJ/kg)
I	Subscript I stands for interface
i, h	Subscripts i and h refer to ice and heater
s, L	Subscripts s and L refer to solid and liquid states
ΔT	Difference between ambient and aircraft surface temperature (K)
Q_{warm}	Energy required to raise the interfacial ice temperature from initial value to 0°C
Q_{min}	Actual required to melt the interfacial ice
Q_h	Energy required to raise the heater temperature from initial value to 0°C

Ahmed Shinkafi is with Aircraft Engineering Department, Air Force Institute of Technology, PMB 2104, Kaduna, Nigeria (Corresponding author: Mobile- +2348087796622, +447423161731, e-mail: a.shinkafi@airforce.mil.ng).

Craig Lawson is with Aerospace Engineering Division,Cranfield University, MK43 0AL, UK.

I. INTRODUCTION

INFLIGHT icing has detrimental effects on the flying characteristics of an aircraft. It decreases lift and thrust, and increases drag and weight. Ice build-up on engine intake could restrict flow into the engine and the ice may breakup and enters inner engine parts which could result in loss of the engine. Ice may also accumulate on control surfaces such as flaps and ailerons which could lead to loss of control. Icing could as well affect pilots' vision and affect the performance of probes [1]. Aircraft icing is caused by super-cooled water droplets striking the aerofoil leading edge and freezing on impact. At present, the thermal ice protection method is the most prominent anti-icing method use in large transport aircraft. The thermal method is mainly divided into the engine bleed hot air and the electro-thermal heater mats systems. Hot air anti-icing systems tap power from the engine which degrades the engine performance and results in high fuel consumption, turbine temperature and, CO_2 and NO_X emissions. This has negative effects on air transport economics, and the environment. In Europe alone, it was estimated that more than 300,000 tonnes of CO_2 are generated daily from aircraft operations [2]. Thus, there is a growing demand for new technologies and flight procedures that would enable aircraft operators to burn less fuel and reduce the adverse effect of aviation to the environment.

Electro-thermal de-icing method is one the leading technologies considered for minimising aircraft in-flight ice protection power requirement. Meanwhile electro-thermal power which is provided by the on-board generators could be quite excessive in terms of weight and fuel consumption. The concept of cyclic de-icing was developed in previous works and is still at different stages of investigation. At the moment there is no single commercial aircraft certified to use this technology for in-flight ice protection. Cyclic electro-thermal de-icing power requirement is a function of the impingement limits, power available and the total cycle time. According to [3], the most efficient removal of ice should be accomplished with 2-3 s of heat on time. This would however, result in many heater elements leading to increase weight and timer complexity. Hence, it was suggested that a power input of 34 kW/m^2 operated using 5% heater-on/off cycle would give a good de-icing performance depending on heater construction

[4]. However, such power would not be available for de-icing in a future next generation aircraft where all aircraft systems will be integrated into one electrical power source.

Reference [5] shows 10% to be the most conservative estimate for heater-on/off cycle; whereas, [6] shows that actually, an electro-thermal de-icer may require just 1% of the energy requirement of a conventional thermal de-icer when fully optimized. The above three results were inconsistent in their findings with regard the optimum power requirement of an electro-thermal de-icing system. It further shows electro-thermal de-icing process is still an open problem. Previous studies developed state-of-the-art methods for de-icing power estimation. These methods however, did not consider the effects of radiation in the heat transfer analysis. However, at higher ΔT, energy exchange due to radiation between aircraft outer surface and surroundings could rise significantly. The objective of this work therefore is to develop an enhanced method for conceptual sizing of an electro-thermal de-icing system based on the full complement of heat transfer mechanisms which would meet the severest icing condition the aircraft is anticipated to encounter. This would provide an efficient yet a conservative power budget required for more-electric aircraft of the future.

II. Ice Protection System Design Regulations

At present, the primary design consideration is Appendix C of 14 CFR Part 25/CS 25.1419 which defines the cloud parameters and the ranges of values required to certify aircraft for flight in known or forecast icing conditions. Appendix C, gave two sets of conditions: the Continuous Maximum (CM) for Stratiform clouds, and the Intermittent Maximum (IM) for Cumuliform clouds icing envelopes; each as a function of LWC vs MVD, and ambient temperature vs pressure altitude. The objective of Appendix C is to provide maximum probable (99%) icing conditions that could be encountered that an aircraft ice protection system (IPS) must be able to cope with.

Currently, no aircraft is certified to fly in icing condition outside Appendix C envelope, i.e., beyond 50μm cloud water droplets size or freezing drizzle and freezing rain [7]. It is regulated that aircraft must exit such conditions as soon as possible if ice protection system is certified in accordance with CS/FAR part 25 Appendix C [8].

III. Aircraft Ice Protection Systems Technology

An aircraft IPS is operated either in anti-icing mode or de-icing mode. In anti-icing mode, the system is operated continuously or intermittently whereas in de-icing mode, the system is operated only when the accretion passed a pre-determined level. The three different ice protection methods have different requirements. Chemical de-icers work by applying aircraft de-icing fluids on the surfaces to inhibit or delay the reformation of ice. The fluids serve as icing inhibitors by preventing the adhesion of ice to the protected surface or making mechanical removal easy. These fluids operate by lowering the freezing point of water on a protected surface so that it does not freeze on the surface during contact.

Mechanical de-icers work on the principle that ice is naturally stiff and brittle, slight distortion therefore fractures it. The shattered ice residues are then swept away by aero forces. For this reason, mechanical de-icers operate in de-icing mode only as the ice must be allowed to build-up to an acceptable limit before breaking its adhesion to the surface. A typical example of mechanical IPS is the Pneumatic Boot system. This technology has the list energy requirement among all in-flight anti/de-icing technologies. It is however associated with uncertainties and structural fatigue in some cases. Hence, they are normally limited to low-to-mid speed application for fear of deformation on the wing aerofoil or intake leading edge.

Thermal anti/de-icing system is one in which heat is used either to prevent ice from building up or to remove it once it accumulates over protected surfaces. Basically, the objective of the thermal IPS is to provide heating to the protected surfaces such that their temperatures remain over and above the freezing point of water or at least, come up periodically to dislodge an accumulated ice. Among the three traditional de-icing methods mention above, only the thermal method cleans the protected surface well enough without undue structural fatigue/damage and environmental pollution. The problem of the thermal system is that it impedes the performance of the engine because of the shaft-power off-take or bleeds air off-take. This impediment is compensated for by excess fuel consumption which in turn increases direct operating cost and gas emission. Thermal IPS can be engine bleed hot air or electrically operated.

There are two types of thermal melting namely: evaporative and running wet system. In an evaporative system, high energy fluxes are used which evaporates all impinging droplets leaving the downstream surfaces dry. In a running wet system, a low energy flux is applied allowing the liquid droplets run back in a thin liquid film on the surface. Evaporative system requires high energy whereas the wet system risks runback icing which may require yet another cycle of de-icing.

IV. Current Electro-Thermal De-Icing Methods

The principle of the electro-thermal IPS is to transfer the energy required for anti/de-icing to the protected areas in electrical form. There are three major classifications of this technology namely, microwave energy, heater mats and laser de-icing systems. Microwave de-icers work by raising the droplets temperature such that they do not freeze on contact with aircraft surface. Energy losses are great in this method because only a fraction of the microwave energy is intercepted by the protected surface.

In heater matde-icers, heater elements are installed on the protected surfaces and energized by electricity to produce the desired heat. The advantages of this technology are that the heater element can be tailored to suit the application which minimizes wastages as heat is directed at the protected surfaces alone. Its dis-advantages are that it is relatively heavy and expensive because large electrical power is required to activate the system.

Use of lasers for inflight de-icing is a more recent technology and is still under development. In this technology, a beam of radiant energy is generated and directed towards critical surfaces to create a footprint on that surface of the aircraft. The beam is manipulated so that the footprint is moved about on the aircraft surface to remove ice. Laser beams have wavelengths that are reflected by aircraft surface and absorbed by ice. The absorbed beam generates heat that removes the ice as the beam footprint is moved about. Laser beam generators could be heavy but mirrors could be used repeatedly to reflect the beam unto a wider area than can be covered by the generated beam [9].

V. Review of Previous Works

In 1996, an experimental program was carried out by Al-Khalil [5] at NASA icing research tunnel to validate the electro-thermal capabilities of ANTICE and LEWICE/Thermal codes by direct comparison of experimental and predicted temperatures using electrically heated NACA0012 aerofoil. The second part of that research was led by W.B Wright [10] in 1997. In 2003, Petrenko [11] developed a simple Pulse Electro-thermal De-icing model. In that study, Petrenko demonstrated that the de-icing energy is linearly proportional to the inverse power density. The system is energized by pulsating the current follow into it for some milliseconds. In this method, the interfacial ice is broken or melted leaving the upper layers of the ice to be removed by the action of external forces such as drag, gravity and free stream flow. Petrenko [6] indicated that a pulse de-icer may require just 1% of the energy requirement of a conventional thermal de-icer when fully optimized. Botura et al. [12] developed a low thermal mass and low energy system with an average power density of less than 1.5W/in^2 at -4 degrees Fahrenheit. Paul Stoner et al. [13] described a methodology for fabricating a Ti-Ni heater element and its electrical energy controller.

Goodrich Corp tested electro-thermal technology on a Cessna 303T wing leading edge during the 2003/4 winter, and reported that between 20-50% energy was saved compared to conventional electro-thermal method [12]. The B787 heater mats were developed by GKN Aerospace based using composites materials. The B787 power consumption was reduced to between 45 to 75kW using this technology compared to 150 to 200kW required if classical technology was used [14]. In 2010, Habashi[15] introduced volumetric source term within the conduction layer in FENSAP-ICE CHT module for heater pads energy simulation. In mid-2010, Meier and Schlz [16] used SAE AIR/1168/4 [3] method for estimating cyclic de-icing power to develop a simple model for estimating electro-thermal de-icing energy.

A. Modeling of Electro-thermal De-icing System

1) Analytical Method

The value of the de-icing system heat flux is a major determinant in the design of the heating system. Reference [17] developed a model for low power operation of an electro-thermal de-icer. According to this method, the total time (t) it takes to raise the temperature of ice from temperature T to the melting temperature (T_{melt}) is given by:

$$t = \frac{\pi(T_{melt}-T)^2}{4*\dot{q}_{anti}{}^2}(\sqrt{\lambda_i\rho_i c_i} + \sqrt{\lambda_s\rho_s c_s})^2 \quad (1)$$

and the total energy required to de-ice the wing is given by:

$$Q = Q_{warm} + Q_{min} + Q_h \quad (2)$$

This was expressed as:

$$Q = \frac{\pi(T_{melt}-T)^2}{4W^2}(\sqrt{\lambda_i\rho_i c_i} + \sqrt{\lambda_s\rho_s c_s})^2 + d.\Delta H_{f,ice}\rho_i + d_h.C_h.\rho_h \quad (3)$$

The above method was based on using a thin-film heater and shortening the heating time to minimise heat exchange between the heater and the environment.

2) Numerical Method

Reference [18] developed a model based on finite difference method to evaluate the minimum power required for ice layer de-icing. The problem was solved using four equations: heat transfer equation of heater and substrate of the aerofoil, ice and the enthalpy. A one-dimensional transient heat conduction equation is given by:

$$\rho c_p \frac{\partial T}{\partial t} = \frac{\partial}{\partial x}\left(k\frac{\partial T}{\partial x}\right) \quad (4)$$

The thermal conductivity, density and heat capacity were constant over the model domain; hence (4) was simplified as:

$$\rho_j c_j \frac{\partial T_j}{\partial t} = \lambda_j \frac{\partial^2 T_j}{\partial x^2} + q_j \quad (5)$$

In the case of the interfacial layer, this was given by:

$$\frac{\partial H_1}{\partial t} = \frac{\partial}{\partial x}\left(k_1\frac{\partial T_1}{\partial x}\right) \quad (6)$$

where H1 is the enthalpy, T1 is the temperature and k1 is the thermal conductivity of ice. The enthalpy was given as:

$$H_1 = \begin{cases} \rho_s c_s T_1, T_1 < T_m \\ \rho_L c_L(T_1 - T_m) + \rho_L(c_s T_m + \gamma),\ T_1 > T_m \end{cases} \quad (7)$$

$$k = \frac{\mu L}{\lambda} \quad (8)$$

The boundary conditions at the interface were given by:

$$T_j \mid_I = T_{j+1} \mid_I \quad (9)$$

$$k_j \frac{\partial T_j}{\partial x} \mid_I = k_{j+1} \frac{\partial T_{j+1}}{\partial x} \mid_I^{j=1,2} \quad (10)$$

where the initial conditions are $T_j = T_0$ and $j = 1,2,3$. This method was used to simulate the heat transfer between the heater and the environment.

B. Cyclical Electro-thermal De-icing

Reference [16] presented a simple method for assessing the cyclic power demand. Based on this method, the overall collection efficiency (E_m) for 20μm MVD can be calculated using:

$$E_m = 0.00324 * (\frac{v}{t})^{0.619} \quad (11)$$

$$\dot{m} = v * t * LWC * E_m \dot{q}_{sensible} = \dot{q}_{cyclic} = \frac{\dot{m}_{ice}}{t}[\Delta T c_i + L_f] \quad (12)$$

where $\dot{m}_{ice} = t.\rho$ and the average specific heat flux is given by:

$$\dot{q}_{total} = \dot{q}_{PS} * k_{PS} + q_{cycl} * k_{cycl} \quad (13)$$

where k_{PS} is the ratio of the area to be de-iced by the parting strip to the total protected area (for initial design this is taken as 19%). K_{cycl} is the ratio of the cyclic heat on time to the total cycle time.

VI. Current Approach

De-icing power can be optimized by combining the cyclic de-icing and pulse electrical de-icing methods. The cyclic de-icing method is basically used to decrease the continuous heated area, heat-on-time, and the heat drainage into ice or the structure. The method allows for the calculation of the relative portion of the parting strip area for anti-icing with respect to the overall area of the surface to be protected. The remaining is then de-iced cyclically. The problem with this method is to know the allowable ice thickness and the heat on and off periods for efficient performance. This problem could be solved using the pulse de-icing method. However, other important factors contributing to energy loss have to be accounted. The present work therefore utilises a combination of cyclic and pulsing de-icing techniques factoring radiation along with convection and conduction losses.

A. Wing De-icing Modelling Process

The wing de-icing modelling process used in this work is as shown in Fig. 1.

1) De-icing Parameters

Table I shows important aircraft parameters used in developing the model which is configurable for any medium to large fixed wing aircraft.

TABLE I
Aircraft Parameters

Parameter	Value
Engine pod diameter	1.7m
Medial wing Leading edge sweep (φ_{LE})	25°
Probes protected area	0.47 m^2
Slat 4 L_{MAC}	2.5m
Wing body setting angle (α)	3.66°
Wing gross area	122.4m^2
Wing Mean Aerodynamic Chord (L_{MAC})	3.16m
Wing L_{MAC} thickness	12.50%
Wing Span	34.1m
Wing total protected area	5.7m^2

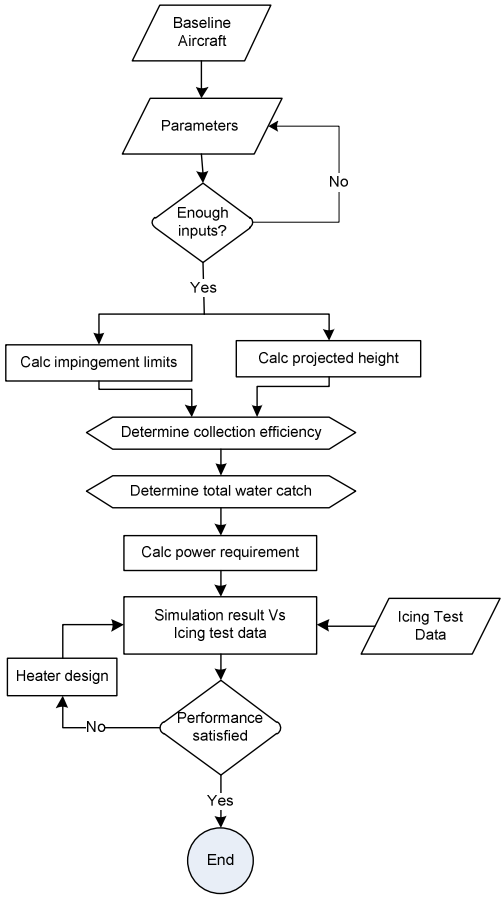

Fig. 1 Detailed Modelling Process

2) Design Point

According to the above design standards, the design limits of the de-icing system are as follows:

- the cloud LWC is above 0.14g/m^3
- the air temperature or aircraft surface is below 0°C
- the air temperature is above -40°C
- 15μm ≤ MVD ≤ 50μm
- aerofoil NACA 65$_1$-212

3) Impingement Limits

In estimating the anti-icing power required it is necessary to establish the limits of water impingement on the surface. The impingement limits describe the upper (S_u) and lower (S_l) limits of the protected area. To optimize the energy distribution, there is the need to determine the extent of protection both span-wise and along the chord. Using a mean aerodynamic chord of 3.16m for Appendix C CM icing condition, the impingement limits for the upper and lower surfaces were calculated using (14)-(17). Reference [19] presents curves for determining the impingement limits for several aerofoil sections at various angles of attack. Therefore, the corresponding values of the DRR were read relative to the calculated droplet Reynolds number.

$$S_U/S_L = f(K_0) \quad (14)$$

The inertia factor *K*was calculated from:

$$K = \left[\left(\frac{1}{18}\right).\frac{d_{med}^2.V_{TAS}.\rho_{water}}{\mu_{icing}.L_{MAC}}\right] \quad (15)$$

$$K_0 = DRR.K \quad (16)$$

but $DRR = f(Re)$, and

$$Re_d = \frac{d_{med}.\rho_{icing}.V_{TAS}}{\mu_{icing}} \quad (17)$$

The values of S_U and S_L were evaluated for different droplet sizes and 4° body angle of attack as shown in Fig. 2.

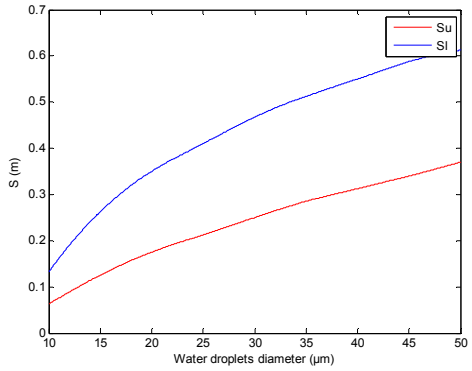

Fig. 2 Impingement limits

4) Heater Design Considerations

To calculate the energy balance on the surface of the aerofoil, a typical heater mat arrangement was modelled as illustrated in Figs. 3-5. The upper surface of the heater is made of a thin layer of Neoprene which serves as electrical insulator and erosion shield. Neoprene's excellent chemical, oil, water and solvent resistance made it a suitable erosion shield. The sprayed heater element is sandwiched by thin layers of GRP for stiffness. Another thick layer forms the inner layer of the heater mat. This layer doubles as electrical insulator and thermal insulator. The outlined lower layer represents the aerofoil structure.

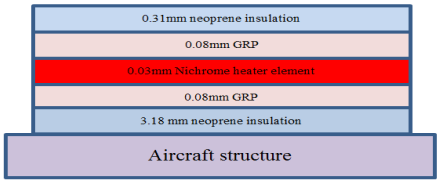

Fig. 3 Layout of heater mat model used for the calculation

A maximum heater ribbon thickness of 6.35mm was used with a gap of 1.27mm analysis based on recommended heater design guidelines in [3] and [20]. The stagnation line does not have a fixed location over the leading edge. It is a function of the body setting angle and aircraft attitude in flight. Therefore, in order to cover the range of the stagnation line, a 30mm parting strip width was used. The heater mat upper and lower bounds were based on impingent limits shown in Fig. 2. Each heater mat span-wise length is given by the slat length.

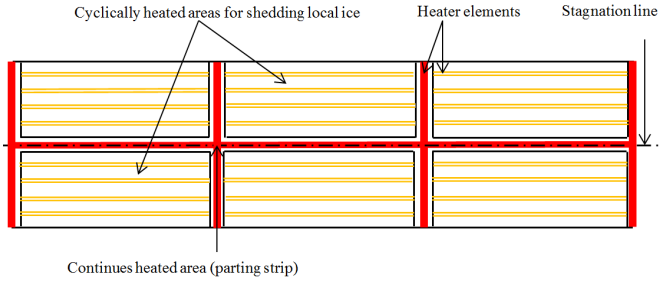

Fig. 4 Leading edge heat mat layout

Based on the a slat length shown in Table I and the impingement limit analysis, a total of 125 heating zones and 4 four break points per slat were used in addition to the parting strip.

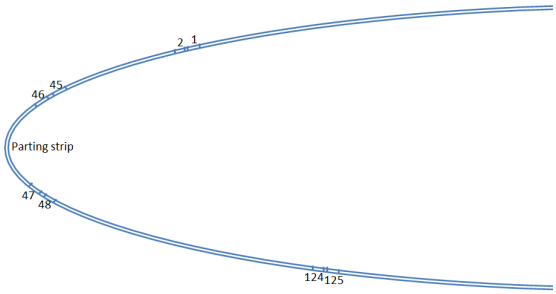

Fig. 5 Locations of heater elements

B. De-icing Energy Calculation

In the present study, the radiation and conduction through composites were added and the process re-evaluated with a view to see the effect on the optimum de-icing power. The new approach is represented by (18):

$$P_{de-icing} = q_{conv} + q_{rad} + q_{cond} \quad (18)$$

The Newton's law of cooling states that the rate of cooling of the surface of a solid, immersed in a colder fluid, was proportional to the difference between the temperature of the surface of the solid and the temperature of the cooling fluid. In other terms this is referred to as convective cooling which can be expressed by the following equation:

$$q_{conv} = U(T_s - T_\infty) \quad (19)$$

Heat transfer from the heater due to net radiation exchange (q_{rad}) with the surroundings is given by:

$$q_{rad} = \varepsilon\sigma(T_s^4 - T_0^4) \quad (20)$$

Thermal conduction is described by Fourier's Law of heat conduction as follows:

$$\frac{\Delta q}{\Delta t} = -kA\frac{\Delta T}{\Delta x} \quad (21)$$

where A is the area of the cross section through which heat is conducted, k is the thermal conductivity, ΔT is the temperature difference between the two points that are separated by a distance x, and $q$is the transferred amount of thermal energy within time$t$[21].Hence heat transfer due to conduction from the heater to the laminates is given:

$$q_{cond} = \frac{k(T_s - T_\infty)}{x} \quad (22)$$

Thus, (18) becomes:

$$P_{de-icing} = U(T_s - T_\infty) + \varepsilon\sigma(T_s^4 - T_\infty^4) + \frac{k(T_s - T_b)}{x} \quad (23)$$

Therefore the overall heat transfer coefficient represented by U can be expressed as:

$$\frac{1}{U} = \frac{1}{h_s} + \frac{x_{GRP(i)}}{k_{GRP}} + \frac{x_{GRP(o)}}{k_{GRP}} + \frac{x_{N(i)}}{k_N} + \frac{x_{N(0)}}{k_N} + \frac{x_C}{k_C} \quad (24)$$

The termh_s can be calculated from the following empirical relation:

$$h_s = Nu.\frac{k}{x} \quad (25)$$

The Nusselt number Nu, is given by:

$$Nu = 0.0296.Re_x^{0.8}.Pr^{0.4} \quad (26)$$

where Prandtl (Pr) and Reynolds' (Re) numbers are dimensionless quantities that could be calculated from the following relationships:

$$Pr = \frac{C_p.\mu}{k_0} \quad (27)$$

$$Re = \frac{\rho_{MSL}.V.l}{\mu} \quad (28)$$

VII. Model Performance Verification and Validation

Consider a small aircraft flying in a known icing condition of -10°C at a speed of 100 kt. It would take the aircraft (t_{icing}) to exit the icing encounter.

$$t_{icing} = \frac{S_{horizantal}}{V_{TAS}} \quad (29)$$

Using (16) on CM icing condition, it would take the aircraft 600 s to exit the icing encounter. Supposing ice has to be removed once it reaches 1mm thickness by a heater element ofthickness 0.03mm on a composite aerofoil of thickness 2mm with the material values shown on Table II.

TABLE II
Material Properties

Layer	λ (W/m.°C)	ρ (kg/m^3)	c (J/kg.°C)	d (mm)
Ice	2.5	920	1882	1
Heater	11.3	8400	450	0.03
Neoprene	0.19	1250	1200	3.49
GRP_{out}	0.35	1900	670	0.18
GRP_{in}	0.35	1900	670	2

The peak power was obtained by solving (23) and multiplying with the total area covered by cyclic de-icing. The total energy consumed was calculated from the sum of parting strip power and cyclic power.

A. Overall Heat Transfer Coefficient

Using (12), the plot of the values U at different locations along the aerofoil for both laminar and transient flows is shown in Fig. 6.

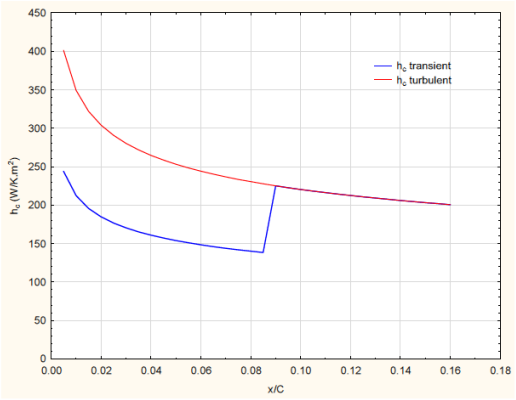

Fig. 6 Plot of overall heat transfer coefficient for both laminar and turbulent flows

B. Surface Distance along the Chord

In estimating the heating intensity along the chord, two parameters have to be used simultaneously. These are the ambient temperature and clouds liquid water cont. Thus. the energy balance at every point on the aerofoil, for three different icing conditions 0°C/0.8gm^{-3}, -15°C/0.5gm^{-3} and -30°C/0.2gm^{-3} was conducted. Variation of the surface heating intensity with distance along the chord could be used to optimise the heater operation. This is because the maximum power is not required throughout the length of the aerofoil. To optimise the heater operation, we need to determine the heating intensity along the chord. Fig. 7 shows how the heating requirement decays along the chord reference to upper surface.

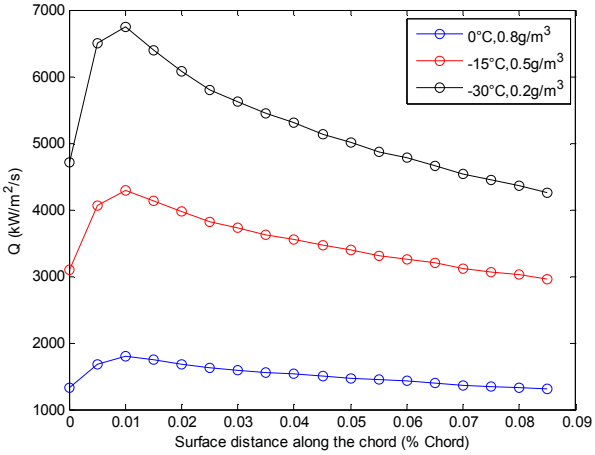

Fig. 7 Required heat intensity along the chord

It should be noted that 0.8g/m^3 clouds water concentration corresponds to an ambient temperature of 0°C even though this level of surface heating does not provide 100% evaporation. Therefore, if the objective is to evaporate the entire surface water, -30°C/0.2gm^{-3}case has to be taken as the critical design point.

C. Power Density

Fig. 8 shows the corresponding values of power density for 'convection term only' and 'convection plus radiation and conduction' for different chord-wise locations along the aerofoil.

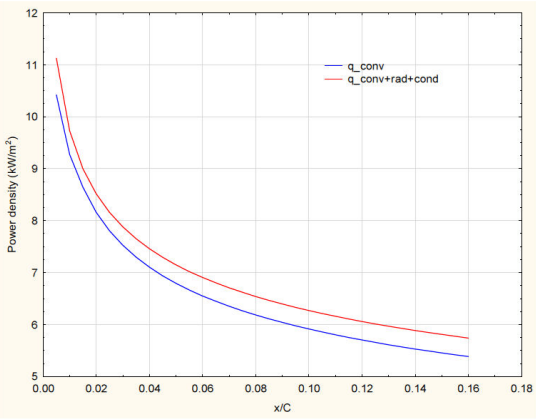

Fig. 8 Values of power density for laminar flow at different locations along the chord

Using the matching plot technique, the power and energy curves were plotted on the same graph sheet as presented in Fig. 9.

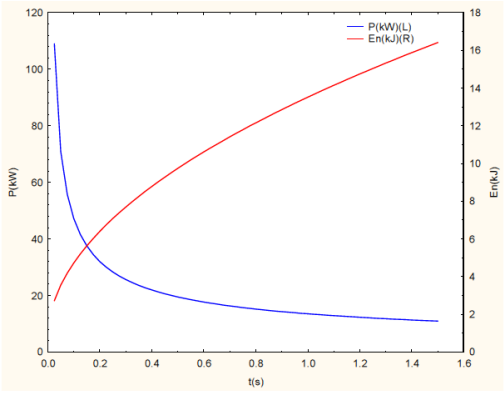

Fig. 9 Plot of de-icing power against energy consumption for different pulse rates

The region below each graph satisfies the performance requirements. The above approach idealises the variations of the power and energy costs with pulsing time. The point of intersection of the two curves gives the optimum pulse time for a given ice thickness and therefore makes the design point with respect to heat on time. Hence, the corresponding value on y-axis gives the design power for the pulse de-icer.

The performance of the model was compared with an experimental result presented in [10] using 0.2s pulsing time in every 100s cycle.

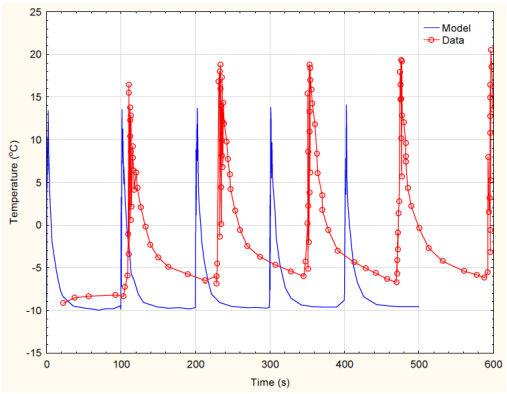

Fig. 10 Response of the skin temperature to heating time

The performance of the model compares very well in terms of cyclic de-icing process as shown in Fig. 10.

VIII. Summary

An enhanced method for sizing aircraft electro-thermal de-icer has been presented. The method took into account the three primary heat transfer mechanisms, and heater efficiency. The performance of the model compared well with experimental results.

References

[1] Gent, R. W., Dart, N. P. and Cansdale, J. T. (2000), "Aircraft Icing", The Royal Society, , no. 358, pp. 2873-2911.
[2] SESAR (2012), SESAR Releases: Advancing ATM Modernisation, available at: http://www.sesarju.eu/news-press/news/sesar-releases-advancing-atm-modernisation-1055 (accessed 03/26).
[3] SAE Aerospace (1989), Ice, Rain, Fog, and Frost Protection, AIR1168/4, Society of Automative Engineers, Inc, PA.
[4] Shinkafi, A. and Lawson, C. (2013), "Evaluating Inflight Ice Protection Methods for Applications on Next Generation Aircraft", Journal of Aerospace Engineering and Technology, , no. 2231-038X.
[5] AL-Khalil, K. M., Horvath, C., Miller, D. R. and Wright, B. W. (2001), Validation of NASA Thermal Ice ProtectionComputer Codes, Part 3: The Validation of Antice, NASA/TM-2001-210907, NASA, Washington.
[6] Petrenko, V., (2006), Method for Modifying Friction Between an Object and Ice or Snow (Patent No. US 7,034,257), 219/482 ed., H05B 3/02, Hanover/US.
[7] Moir, I. and Seabridge, A. (2008), Aircraft Systems Mechanical, Electrical, and Avionics Subsystems Integration, 3rd ed, Wiley, New Jersey.
[8] FAA (2007), Pilot Guide: Flight in Icing Conditions, 91-74A, FAA.
[9] Palacios, J. L. (2008), Design, Fabrication, and Testing of an Ultrasonic De-icing System for Helicopter Rotor Blades (PhD thesis), The Pennsyvania State University, PA.
[10] Wright, B. W., Al-Khalil, K. and Miller, D. (1997), Validation of NASA Thermal Ice Protection Computer Codes Part2 - LEWICE/Thermal, AIAA 97-0050, AIAA, Virginia.
[11] Petrenko, V. F., Higa, M. and Starostin, M., Deresh, L. (2003), "Pulse Electrothermal De-icing", in Chung, J.S., Prinsenberg, S. (ed.), Proceedings of The Thirteenth (2003) International Offshore and Polar Engineering Conference, Vol. 1, 25-30 May 2003, Honolulu, Hawii, USA, The International Society of Offshore and Polar Engineers, Honolulu, pp. 435.

[12] Botura, G. C., Sweet, D. and Flosdorf, D. (2005), Development and Demonstration of Low Power Electrothermal De-icing System, AIAA 2005-1460, AIAA, Washington.
[13] Stoner, P., Christy, D.P. and Sweet, D.B., (2007), Low Power, Pulsed, Electro-thermal Ice Protection System, 244/134 D ed., B64D 15/4, USA.
[14] GKN (2010), Composite Aircraft Wing Research gets underway at GKN Aerospace, available at: http://www.gknaerospace.com/newsarticle.aspx?page=S633463542178688750&ArchiveID=5&CategoryID=33&ItemID=313&src= (accessed 05/15).
[15] Habashi, W. G. (2010), Recent Progress in Unifying CFD and In-Flight Icing Simulation, ICFD10-EG-30I11, ICFD, Ain Soukhna, Egypt.
[16] Meier, O. and Scholz, D. (2010), A Handbook Method for the Estimation of Power Requirements for Electrical De-icing Systemms, 161191, Hamburg University of Applied Sciences, Hamburg, Germany.
[17] Petrenko, V. F., Charles, R. S., Kozlyuk, V., Petrenk, F. V. and Veerasamy, V. (2011), "Pulse Electro-thermal De-icer (PETD)", Cold Regions Science and Technology, , no. 65, pp. 70-78.
[18] Qinglin, M. (2010), Aircraft Icing and Thermo-Mechanical Expulsion De-icing Technology (unpublished MSc thesis), Cranfield University, Cranfield.
[19] Bowden, D. T., Gensemer, A. E. and Skeen, C. A. (1964), Engineering Summary of Airframe Icing Technical Data, FAA ADS-4, FAA, Washington, D.C.
[20] Lewis, J.P, Bowden, T. (1952), Preliminary Investigation of Cyclic De-icing of an Airfoil using an External Electric Heater, RM E51J30, NACA, Washington.
[21] Xie, A. (2012), Interactive Heat Transfer Simulations for Everyone, , The Concord Consortium, VA, USA.